Enhanced Diffusion in Active Intracellular Transport

Avi Caspi, Rony Granek, and Michael Elbaum
Department of Materials and Interfaces, Weizmann Institute of Science, Rehovot 76100, Israel
(Received 16 March 2000)

We show that within a living eukaryotic cell, mean square displacement of an engulfed microsphere shows enhanced diffusion scaling as $t^{3/2}$ at short times, with a clear crossover to subdiffusive or ordinary diffusion scaling at longer times. The motion, observed nearby the nucleus, is due to interactions with microtubule-associated motor proteins rather than thermal Brownian motion. We propose that time-dependent friction introduced by the intracellular polymer networks leads to sub-ballistic motion, analogous to subdiffusion observed in passive networks of semiflexible biopolymers.

PACS numbers: 87.17.–d, 83.10.Nn, 87.16.Ka

Biopolymer gels making up the cytoskeleton of eukaryotic cells have been the subject of many *in vitro* experimental and theoretical studies [1]. These semiflexible polymers, in particular, microtubules and filamentous actin (f-actin), are rigid enough to distinguish between longitudinal and transverse directions at the level of the individual polymer. Thermally driven bending modes of the polymers lead to anomalous diffusion phenomena of particles embedded in gel networks [2] or attached to single filaments [3]. Within the living cell the microtubules and f-actin associate with dissipative motor proteins to generate directed forces, resulting in production of mechanical work and dynamic transport processes. Microtubules and the motor families kinesin and dynein are largely responsible for spatial organization of intracellular structures and for the transport of cargo between different compartments. Actin filaments and the myosin family of motor proteins are primarily associated with cellular attachments, contraction, and motility. Within the living cell the motion of transported vesicles is typically saltatory, suggesting simultaneous operation of several motor types. The current work addresses active transport within the intracellular microrheological environment.

A particle embedded in a network of semiflexible polymers displays a mean square displacement $\langle x^2 \rangle$ (MSD) which follows a power law of $t^{3/4}$, rather than linear time dependence for a Brownian particle. This was first demonstrated by tracing the motion of microspheres embedded in a gel of purified actin filaments, using video microscopy [2]. Using diffusive wave spectroscopy it was possible to detect the $t^{3/4}$ scaling over many decades in time [4]. It was also shown that this power law is obtained for both the longitudinal and transverse motions of a single actin filament embedded in an actin gel [5]. The shear modulus for entanglements in a solution of semiflexible actin has a high frequency $\omega^{3/4}$ scaling, in contrast to $\omega^{1/2}$ scaling for flexible polymer solutions [6]. The particle studies are in agreement with earlier light-scattering measurements [7].

Several experimental studies using intracellular probes have focused on the estimation of the cytoplasmic viscosity. Using size-fractionated Ficoll, it was shown that diffusion inside the living cell is hindered in a size-dependent manner [8]. The translational diffusion of nanometer-sized beads has also been measured inside living cells by fluorescence correlation spectroscopy [9]. Using micron-sized magnetic beads, the viscoelasticity was obtained by measuring the probe response as a function of the applied field [10].

In order to study microrheology within living cells, we track the motion of polystyrene microspheres, 3 μm in diameter, inside living fibroblasts using video-based methods. Cells were observed in Petri dishes with glass bottoms and maintained at 37 °C during experiments. Measurements were made on an inverted microscope equipped with an oil-coupled $\times 100/1.3$ NA Zeiss Fluar objective, and a $1/2$ in. digital CCD video camera (with $\times 0.5$ lens; 160 nm/pixel). The beads were coated on their surface by the lectin concanavalin A so as to adhere to the cell membrane. They were introduced into cells either by incubation with the cell culture during introduction of cells into the observation chamber, or by direct placement on the cell surface near the edge using optical tweezers. In both cases the beads were engulfed into the internal volume of the cell and carried toward the center, i.e., the region occupied by the nucleus. All measurements presented here were made in this central part of the cell, Fig. 1. We verified by scanning electron microscopy and fluorescence confocal microscopy on fixed samples that the beads are indeed topographically inside the cell [11]. Measurements were made on cells of the human-derived SV80 fibroblast line (11 samples), with some on multinuclear giant cells [12] of the same line (six samples), and on murine NIH 3T3 cells (two samples).

In the central perinuclear region the bead motion appears to be random within a restricted area. The motion

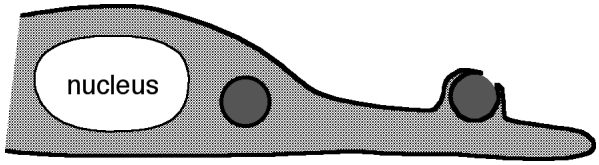

FIG. 1. Cross-sectional sketch of a cell showing one bead in the perinuclear region where measurements are made, and the other in the process of engulfment into the cell volume.

0031-9007/00/85(26)/5655(4)$15.00

was recorded for several minutes (5000 to 12 000 frames) by direct digitization in a personal computer at a rate of 25 frames/s. Bright-field imaging was used for particle tracking while differential interference contrast was best for cell observation. A correlation algorithm was used to locate the position of the bead to subpixel resolution [13]. (A bead fixed to the glass shows a positional uncertainty of <20 nm.) The raw data are coordinate lists of the bead's projection in the plane. The two-dimensional MSD is computed as a time average for individual trajectories. Stationarity was verified by evaluation of truncated and subsampled data sets.

Results from two typical cases are shown in Fig. 2a. At short times, we observe enhanced diffusion $\langle x^2(t)\rangle \sim t^\gamma$ where $\gamma = 1.47 \pm 0.07$, from 19 particles. The amplitude of the motion varies widely, such that $\langle x^2(t = 1\ \mathrm{s})\rangle^{1/2}$ ranges from 0.09 to 0.18 μm. The enhanced diffusion regime ends at a time scale $\gtrsim 1$ s. As seen in the inset, the particle trajectory maintains directionality over a longer time scale. Within the short-time regime where the MSD displays anomalous scaling, however, the probability distribution is nearly Gaussian, centered around zero.

Stochastic processes involving random impulses yield a ballistic regime ($\gamma = 2$) at measurement times short compared to the correlation time of the drive, and diffusive behavior ($\gamma = 1$) at longer times. We are unable to fit the results to equations representing such a crossover (for example, [14]), indicating an unexpected exponent for the active intracellular movement.

We hypothesize that cytoskeleton-based transport activity is responsible for the nonthermal element driving the bead. SV80 cells were treated with specific drugs to disassemble either microtubules or filamentous actin, leaving their associated motor proteins without an extended track along which to move. Nocodazole (three samples, 5 h at 10 μM concentration) was used for microtubule depolymerization, while f-actin was depolymerized using cytochalasin D (three samples, 2–3 h at 0.2 μg/ml concentration). Nocodazole-treated cells show a loss of long-range internal vesicle movements, while cytochalasin treated cells are not motile and are unable to divide. As shown in Fig. 2b, microtubule depolymerization eliminated the enhanced diffusion, while actin depolymerization had no measurable effect. Thus we may conclude that microtubule motors are responsible for the enhanced diffusion and associated anomalous exponent.

The interaction of the probe with the network may be understood by considering its cellular context. The process by which the bead is engulfed into the cell, similar to phagocytosis [15] in which an external body is "cupped" by protruding planar extensions, leaves it surrounded by a layer of plasma membrane, Fig. 1. This membrane shell is clearly visible using the membrane-specific fluorescent dye DiI. Thus the bead is likely to be recognized by its coating and transported by the microtubule motor system within the cell. Microtubules surrounding the engulfed beads were visualized by confocal immunofluorescence microscopy [16], Fig. 3. Note that the filament net surrounds the beads densely, i.e., the network mesh size is much smaller than the bead. Superdiffusive motion ($\gamma > 1$) in such a mesh again indicates the activity of motor proteins, which connect the bead to one or more of the microtubules and drives it through the net formed by the others.

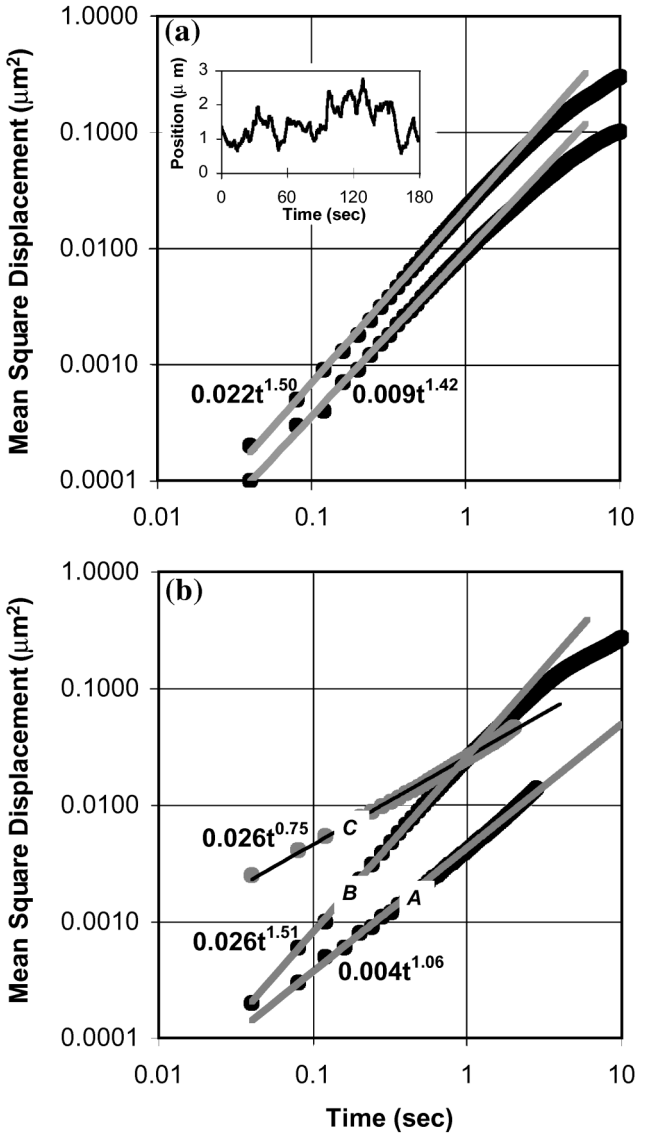

FIG. 2. Measured MSD on beads within living cells. (a) Two typical cases showing enhanced diffusion with a power of 1.5 at short times. Solid lines are fit over the range of 0.04–1.0 s. Inset: a 60 s trajectory along an arbitrary axis. (b) Curves as indicated: (*A*) following depolymerization of the microtubules using nococazole—Brownian diffusion; (*B*) following depolymerization of the actin filaments using cytochalasin D—enhanced diffusion as in untreated cells; (*C*) lipid granules normally inside the cells, without treatment—subdiffusion.

The 3/2 power could represent an enhancement of diffusion. This has been treated theoretically in the context of a random velocity field model [17], where a half-integer power is introduced by the influence of diffusive motion in between ballistic events. This is, however, inconsistent

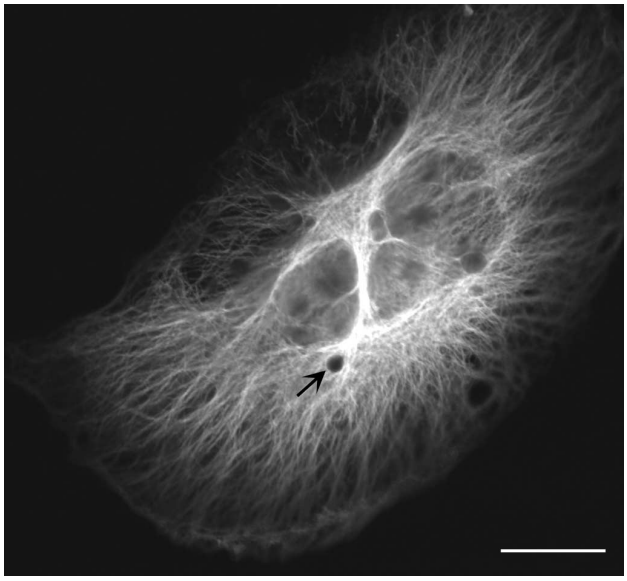

FIG. 3. Immunoflorescence image (Olympus Fluoview confocal microscope, PlanApo ×60/1.4 objective) of a multinuclear giant cell fixed and stained to show the microtubules [16] following measurement on the indicated bead; scale bar 20 μm.

with the inability of an optical trap (20 pN escape force) to stop or hinder the bead movement, as well as with the implications of Fig. 3, which shows that the bead is likely to be influenced by many motors simultaneously.

An insight to the physics underlying the bead movement may be gained by looking at highly refractive, filled lipid spheres or "granules" naturally present in these cells. They are not membrane bound, are not labeled by DiI, and apparently do not interact with motor proteins. In contrast to the beads, they can be held stationary in the optical tweezers for many minutes. Their use as native biological probes of local microrheology has been justified recently [18]. As seen in Fig. 2b, they display subdiffusive scaling $\langle x^2(t)\rangle = at^{3/4}$. The measured prefactor a is comparable to that which would be expected for thermal undulation of microtubule filaments [3,19], taking persistence length 6 mm [20] and solvent viscosity 5 times that of water. Similar scaling is obtained for fluctuations in semiflexible polymer networks *in vitro* [2–5,7], consistent with a picture of the cellular microtubules as a weakly entangled network in which diffusion of the granules is influenced by equilibrium modes of the surrounding filaments. We will argue that a similar microrheological environment is felt by the driven particle.

The non-Newtonian environment inside the cell suggests a self-consistent explanation for the anomalous power based on hindrance to ballistic motion. As the passive diffusion of granules is subdiffusive, the active motion of beads will be sub-ballistic. Our proposal is formalized in the context of the Einstein relation relating driven and thermal processes. A generalization to anomalous diffusion was discussed [21] to explain observations of particles in actin gels, with and without external force [2]. Measured dynamics in the nondriven (thermal) MSD $\langle \vec{x}^2(t)\rangle_{TH}$ define an effective, time-dependent friction $\mu_e(t)$ given by

$$\frac{4k_BT}{\mu_e(t)} = \frac{d}{dt}\langle \vec{x}^2(t)\rangle_{TH}\,, \tag{1}$$

in two dimensions. (More accurately, one should use a memory kernel friction in the context of the generalized Langevin equation [22].) For Brownian diffusion this yields the simple Newtonian viscosity, while subdiffusion in thermal equilibrium with a non-Newtonian environment, as performed by the granules in the cells or by embedded tracer particles in *in vitro* networks, implies time-dependent friction. The $t^{3/4}$ scaling therefore yields $\mu_e(t) \sim t^{1/4}$. Since the driven velocity is $v(t) = F/\mu_e(t)$, one finds that under the action of a force randomly distributed between positive and negative values with variance $\langle F^2\rangle$ and a vanishing mean, the MSD in the driven system, $\langle x^2(t)\rangle_F$, becomes

$$\langle \vec{x}^2(t)\rangle_F = \frac{\langle F^2\rangle}{(4k_BT)^2}\langle \vec{x}^2(t)\rangle_{TH}^2\,. \tag{2}$$

(At very short times, or for vanishing $\langle F^2\rangle$, thermal diffusion adds a contribution $\langle \vec{x}^2(t)\rangle_{TH}$.) Thus the time scaling of effective viscosity yields both the passive $t^{3/4}$ and the active $t^{3/2}$ behaviors.

The proportionality between passive and active components should, in principle, yield a measure of the resultant force acting on the bead. Unfortunately it is not possible to turn on and off the active component. Using the prefactors from thermal diffusion of the granules, and from the driven motion of the beads (Fig. 2), together with the equation above, we find that the resultant force acting on the bead is 2 orders of magnitude smaller than the accepted stall force of a *single* kinesin motor [23], while the rapid escape of the driven bead from the optical trap shows that many motors operate simultaneously. The discrepancy can be explained by noting that "stalled" motors act as pinning sites between the bead and the microtubules. As a result, the action of other motors introduces longitudinal strain. Granules, by contrast, experience effective friction resulting from interaction with transverse undulatory modes of the neighboring filaments. While both transverse and longitudinal thermal fluctuations of semiflexible polymers scale as $t^{3/4}$, the latter are reduced in relative amplitude by the ratio of polymer contour length to persistence length [19], implying that $\mu_e(t)$ for longitudinal response is larger by L_p/L. Correcting the measured passive prefactor by a ratio suitable for microtubules ($\sim 10^{-3}$), the estimated driving force is adjusted upward by 3 orders of magnitude, yielding a reasonable result.

The time-dependent friction also introduces an anomalously low exponent, $\gamma = 1/2$, for times longer than the correlation time of the driving force [22]. While limitations in acquiring very long data sets make it risky to fix an exponent at long times, sampling the data on various time windows permits a test of the domain over which the

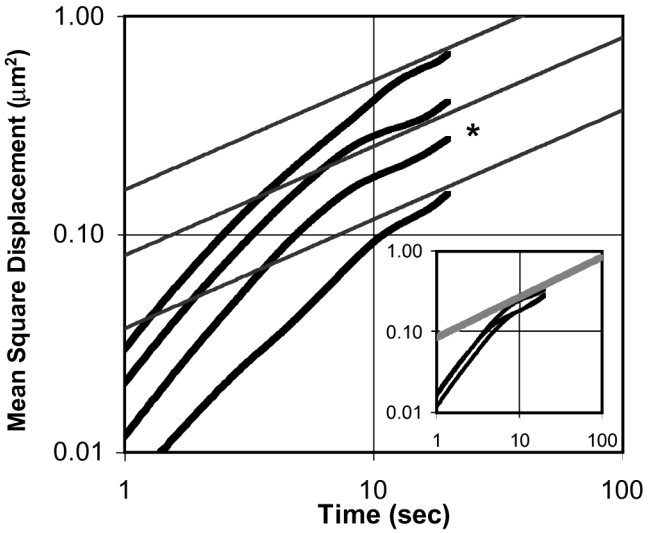

FIG. 4. Four examples showing the trend to subdiffusive motion on the time range from 1 to 20 s. Gray lines display a slope of 1/2. Inset: a comparison between MSD calculated on the data series of the run marked by the *, truncated at 33%, 50%, and 100% of the measurement set (10 000 frames).

MSD is reliable. In many of the resulting analyses the scaling is clearly subdiffusive, as seen in Fig. 4, consistent with the prediction of the generalized Einstein relation. In some cases the subdiffusion regime is not observed, suggesting "loss of memory" in $\mu_e(t)$. Clearly, at times longer than this reinitialization time we expect ordinary diffusion.

In summary, the measurements presented here demonstrate enhanced diffusion with a $t^{3/2}$ power law for an actively transported probe particle inside a living cell, and subdiffusion with $t^{3/4}$ scaling for passively diffusing objects. We propose that the latter is related to the $t^{3/4}$ scaling displayed by particles in networks of purified filaments. The anomalous scaling behaviors can be understood by introducing a time-dependent friction imposed by the non-Newtonian medium in which the motion takes place.

The authors acknowledge essential support from A. D. Bershadsky and members of his laboratory in all aspects of cell biology, and helpful discussions with J. Klafter on anomalous diffusion. This work was supported by the Israel Science Foundation, and by the Gerhard M. J. Schmidt Minerva Center for Supramolecular Architecture.

[1] T. Gisler and D. A. Weitz, Curr. Opin. Colloid Interface Sci. **3**, 586 (1998).
[2] F. Amblard, A. C. Maggs, B. Yurke, A. N. Pargellis, and S. Leibler, Phys. Rev. Lett. **77**, 4470 (1996).
[3] A. Caspi, M. Elbaum, R. Granek, A. Lachish, and D. Zbaida, Phys. Rev. Lett. **80**, 1106 (1998).
[4] A. Palmer, T. G. Mason, J. Xu, S. C. Kuo, and D. Wirtz, Biophys. J. **76**, 1063 (1999).
[5] M. A. Dichtl and E. Sackmann, New J. Phys. **1**, 18 (1999).
[6] F. Gittes, B. Schnurr, P. D. Olmsted, F. C. MacKintosh, and C. F. Schimdt, Phys. Rev. Lett. **79**, 3286 (1997).
[7] E. Farge and A. C. Maggs, Macromolecules **26**, 5041 (1993).
[8] K. Luby-Phelps, P. E. Castle, D. L. Taylor, and F. Lanni, Proc. Natl. Acad. Sci. U.S.A. **84**, 4910 (1987).
[9] K. M. Berland, P. T. C. So, and E. Gratton, Biophys. J. **68**, 694 (1995).
[10] A. R. Bausch, W. Moller, and E. Sackmann, Biophys. J. **76**, 573 (1999).
[11] A. Caspi, O. Yeger, A. D. Bershadsky, and M. Elbaum (to be published).
[12] L. A. Lyass *et al.,* Proc. Natl. Acad. Sci. U.S.A. **81**, 3098 (1984).
[13] J. Gelles, B. J. Schnapp, and M. P. Sheetz, Nature (London) **331**, 450 (1988).
[14] X.-L. Wu and A. Libchaber, Phys. Rev. Lett. **84**, 3017 (2000).
[15] B. Alberts *et al., Molecular Biology of the Cell* (Gerland Publishing, New York, 1994), 3rd ed., p. 619.
[16] Cell where fixed in cold methanol at −20 °C for 15 min, followed by washing with phosphate buffer saline, then stained by a primary antibody for α-tubulin (DM1A) and a secondary rhodamine-labeled antibody.
[17] G. Zumofen, J. Klafter, and A. Blumen, Phys. Rev. A **42**, 4601 (1990); A. Ajdari, Europhys. Lett. **31**, 69 (1995).
[18] S. Yamada, D. Wirtz, and S. C. Kuo, Biophys. J. **78**, 1736 (2000).
[19] R. Granek, J. Phys. (Paris) II **7**, 1761 (1997).
[20] M. Elbaum, D. Kuchnir Fygenson, and A. Libchaber, Phys. Rev. Lett. **76**, 4078 (1996).
[21] E. Barkai and J. Klafter, Phys. Rev. Lett. **81**, 1134 (1998).
[22] The motion of the bead can be described by the generalized Langevin equation in the overdamped limit (written in one dimension)

$$\int_{-\infty}^{t} \mu(t - t')v(t')\,dt' = F(t) + \zeta(t)\,,$$

where $v(t)$ is the particle velocity, $F(t)$ is the driving force, and $\zeta(t)$ is thermal noise whose correlation function obeys the fluctuation-dissipation theorem

$$\langle \zeta(t_1)\zeta(t_2)\rangle = k_B T \mu(t_1 - t_2)\,.$$

[Note that $\mu(t)$ and $\mu_e(t)$ of Eq. (1) are not equal.] For $F(t) = 0$ we obtain, in Laplace space (denoted by $t \to s$), the generalized Einstein relation [24]

$$D(s) = \frac{1}{2}\, s^2 \langle x^2(s)\rangle_{TH} = \frac{k_B T}{\mu(s)}\,.$$

In case of a driven motion, we obtain the relation [21]

$$\langle x(s)\rangle_F = \frac{\langle x^2(s)\rangle_{TH} s F(s)}{2k_B T}\,.$$

For a stochastic force whose correlation function obeys

$$\langle F(t_1)F(t_2)\rangle = \langle F^2\rangle e^{-|t_1 - t_2|/\tau}$$

this yields, at short times $t \ll \tau$, Eq. (2) (replacing, in two dimensions, 2 by 4). For long times $t \gg \tau$, and in our case where $\mu(s) \sim s^{-1/4}$, we find

$$\langle x^2(t)\rangle_F \sim t^{1/2}.$$

[23] K. Visscher, M. J. Schnitzer, and S. M. Block, Nature (London) **400**, 184 (1999); H. Kojima, E. Muto, H. Higuchi, and T. Yanagida, Biophys. J. **73**, 2012 (1997).
[24] H. Scher and M. Lax, Phys. Rev. B **7**, 4491 (1973).